Advances in Science and Technology Research Journal

Advances in Science and Technology Research Journal, 2025, 19(6), 131–139
https://doi.org/10.12913/22998624/202485
ISSN 2299-8624, License CC-BY 4.0

Received: 2025.01.08
Accepted: 2025.04.15
Published: 2025.05.01

Method of photogrammetric processing of scanning electron microscope – images for research of soil microsurfaces

Oleh Ivanchuk[1], Andrzej Mazur[1], Barbara Kępowicz[1*]

[1] Department of Geodesy and Spatial Information, University of Life Sciences in Lublin, ul. Akademicka 13, 20-950 Lublin, Poland

* Corresponding author's e-mail: barbara.kepowicz@up.lublin.pl

ABSTRACT

The paper presents the method of photogrammetric processing of SEM images and the results of its application to determine the spatial coordinates of the points of the microsoil of the forest soil by measuring their SEM images, obtained on SEM Hitachi S800 with a magnification of 1000×. Depending on the magnification (scale) of the SEM images, the accuracy of the method is: for M = 1000× – $m_{X,Y} = \sim 0.1$ µm, $m_{Z(h)} = \sim 1.0$ µm, and for magnification M = 25000× – $m_{X,Y} = \sim 0.01$ µm, $m_{Z(h)} = \sim 0.1$ µm. The article presents an unusual workflow based on processing in Dimicros, as well as examples of graphic interpretation of digital modeling of the forest soil surface microrelief in the form of microplanes with levels and 3D models obtained using the Surfer program. This information allows learning about the physical and mechanical properties of the soil, its structure, and its resistance to erosion, which is important in construction and environmental protection.

Keywords: scanning electron microscope, photogrammetry, reference test object, digital model of microrelief, 3D model.

INTRODUCTION

The photogrammetric method of obtaining quantitative spatial parameters of the microsurfaces of research objects by measuring their digital stereo images obtained on modern scanning electron microscopes (SEM) is widely used in many industries and research [1–3]. In particular, in microelectronics [4], materials science [5–7], mechanical engineering, aircraft construction [8], in the creation of missile and military equipment, in industries that use nanotechnology [9], in research in medicine [10], biology [11–13], agriculture [14], geology [15–17], crystallography [18], soil science [19] and many others. Currently, there is a tendency to use artificial intelligence in machine learning to automate the processing of SEM imaging systems [17, 20, 21].

In this list, studies of soil microsurfaces deserve special attention. Thus, determining the quantitative parameters of forest soil surfaces and their microstructures make it possible to establish their various properties, in particular, resistance to vertical loads and shear, which is important in the construction industry, moisture resistance and others [22]. Determination of the quantitative parameters of the soil surface and their microstructure, also allows establishing soil susceptibility to erosion due to natural factors [23, 24]. Knowledge of the susceptibility of soils to erosion allows making decisions on how to use eroded soils in order to protect them against further degradation. Erosion, especially water erosion, is the cause of a strong degradation of the soil environment [25, 26]. The areas which are most susceptible to erosion are arable land [27], to a lesser extent grasslands [28], and the least affected are forest areas [29]. A number of works have been devoted to the study of soils and geological rocks with the help of SEM [30–32], but this issue remains relevant even today. The scanning electron microscope uses a high-energy electron beam instead of a light beam. "Electron gun" produces a beam of electrons and directs it toward the sample through an electromagnetic lens system and a series of apertures. To avoid scattering the beam on air particles or pollen, the process is carried out in a high vacuum [33].

The main two types of signals can be recognized. Among the reflected imaging signals, some of the electrons are of low energy – secondary electrons (SE), which are recorded by nanometers located close to the sample. SEs give information about the topography of the sample and are useful for detailed surface imaging [34]. Second group of reflected electrons gives information about the sample are beam backscattered electrons (BSE). These have a higher energy than SE. BSE is influenced by the effect of the atomic number of the elements, which makes it possible to show the relative diversity of the sample structure [35, 36].

The main advantage of SEM over optical microscopy is the ability to obtain an image at higher magnification without losing depth of focus, which facilitates analysis of the sample topography [37]. Electron impacts provide information essential for imaging the component under study, so if appropriate detectors are present, additional data (chemical composition, crystal structure, electrical properties) are also acquired for analysis, which are not provided by optical imaging [17, 38, 39]. Other technologies, such as SfM photogrammetry, provide information about the sample structure at only mm level with less detail [24, 40, 41] In addition, the algorithms used in popular digital photogrammetry programs do not allow for changing image processing parameters, are adapted to the geometry of photos in the center projection and are not adapted to SEM, which, for example, generates problems with the lack of model scale [42].

The aim of this work is to familiarize readers with the SEM image processing method, a unique process of generating a microplane and a 3D model in the Dimicros program is proposed in combination with the presentation of the results in the Surfer program. Dimicros was developed by the authors [43] at the Department of Photogrammetry and Geoinformatics of the National University 'Lviv Polytechnic'. It enables to obtain spatial quantitative parameters of research surfaces and present them in the form of digital models of microrelief (DMMR), microplans and 3D models.

TECHNOLOGICAL SCHEME OF THE METHOD

The study used the Dimicros package available to the authors, dedicated to SEM studies. It provides its algorithm and allows editing of all study parameters and adapted to work in an almost orthogonal projection for each point. Then, the measurement results were visualized in the widely available Surfer program, which has a built-in wide set of interpolation methods for generating a regular grid of values, and allows choosing the optimal algorithm for the nature of the input data. It allowed the authors to choose the optimal interpolation method when building the Grid model.

Preparation of SEM and samples

Before SEM imaging, it is necessary to set the vacuum in the column of the scanning electron microscope to the level of $10^{-5} \div 10^{-6}$ PA, as well as make the appropriate settings of individual components of the microscope.

Preparation of samples for SEM-removal consists in their selection, if necessary their freezing, further reduction to certain sizes (~ 10×10×5 mm), spraying with conductive metal (copper, silver, gold ~ 20 nm thick) and gluing 2–3 samples and reference test -object with conductive glue to the goniometric table (diameter 30–100 mm).

One of the best reference test objects is a diffraction grating in the form of a spherical hemisphere matrix (alloy of silver with sulfur arsenic semiconductor – Ag-AsS with a resolution of 1425 lines/mm, which is made by holographic method and applied to a glass base, about 1.5–2 mm thick) (Fig. 1).

Survey of the reference test object

SEM-stereo survey of the surfaces of the test specimens and the reference test object is, as a rule, normal-convergent method. It consists in that first the SEM image of the reference test object and the sample surface is fixed on the SEM monitor screen at the horizontal position of the goniometric table and the selected fixed value of magnification M, and then successively, the same images of the sample surfaces are fixed at the table angles α from 6° to 12°, depending on the surface relief of the sample.

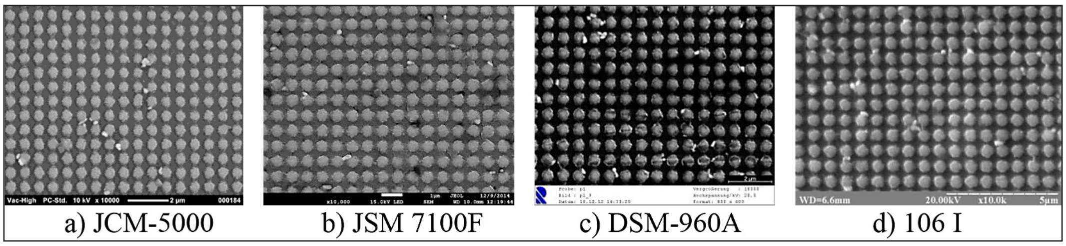

Figure 1. Digital SEM images of a test object with a resolution of r = 1425 lines/mm, obtained on different SEMs with an increase of M = 10000x

In the process of tilting the table, it is necessary to keep the contour of the image in the selected initial position for REM stereo shooting by movements along the *X* and *Y* axes. The basis of removal $b_x = 0$. The goniometric table can be moved along the *X*, *Y*, *Z* REM axes and tilted at angles: α – around the *Y* axis, ω – around the *X* axis, rotated at an angle κ around the *z* axis of the device.

Determining magnification the digital SEM images

Determining the actual magnification values (scale) of a digital SEM image along its x-axis is an extremely important task, as a number of SEMs (DSM-960A, 106I) increase the size of its scale relative to the scale set by a certain fixed factor k during image recording. In particular, for SEM DSM 960A (Carl Zeiss, Oberkochen, Germany) it is k = 1.93085, and for SEM 106I (SELMI, Sumy, Ukraine) - k = 2.8213. SEM Japanese company JEOL (JCM-5000 Neoscope, JSM 710F) capture images in digital form without magnification, i.e. in this case k = 1.0.

In addition, due to the misalignment of the coils of the SEM images, their real scale along the x-axis, y may deviate from the SEM scale up to ± 10%, and it must be taken into account when obtaining quantitative characteristics of research objects. Reference test objects allow seting the actual values of magnification (scale) of SEM images with an accuracy of ± 0.5%.

Therefore, before measuring the REM stereo pairs of research objects, it is necessary to establish their actual magnification and the magnitude of their geometric nonlinear distortion (distortion), which can reach at the edges of the image 120×120 mm to ± 3 mm (~ 30 pixels). After their consideration by polynomial approximation, residual distortions within 0.1–0.3 mm (1–3 pixels). A number of studies of geometric distortions of digital SEM images were performed, which are obtained on SEM of the world's leading companies [30, 44–47]. For their installation (calibration) SEM images of reference test objects (grids, diffraction gratings) with the differences r = 200 lines/mm, r = 1425 lines/mm and r = 3530 lines/mm were used. Measurement of SEM images was performed on a PC using a special program «Test Measuring», which is part of the program «Dimicros» [45], and their effective consideration was performed by a mathematical polynomial of general form of the 3rd degree program «Polycalc». For example, the values of geometric distortions of digital SEM images obtained in Ukrainian SEM 106I at different magnifications are given in the form of vector diagrams before and after their consideration (Fig. 2, 3). Polynomial consideration of distortions allows reducing them by 3-10 times.

Well-known scientists, in particular, Boyde [48], Burkhardt [49], Ghosh [50], Howell [30], Melnyk [32], Shostak [51] studied geometric distortions of SEM images.

Surfaces measurement of microrelief

To perform experimental work, a stereo image of the micro soil of the loess soil (rough, homogeneous) was obtained on the Hitachi S-800 (Japan) at a magnification of M = 1000x and angles of inclination of the goniometric table: left image - $\alpha_l = 0°$, right $\alpha_r = 8°$ (Fig. 4). The real accuracy of determining the spatial coordinates for these survey parameters is $m_{X,Y} = 0.06 \div 0.1$ µm, $m_{Z(h)} = 0.7 \div 1.0$ µm. It depends on the accuracy of measurements of coordinates and parallax points, i.e. on their identification on the stereo pair, which is $m_{x,y,p} = 0.02 \div 0.05$ mm. Measurement of SEM stereo pairs was performed at the Delta SFS using the Stereo SEM program, which is part of the Dimicros software package. Measurements can be performed monocularly on a regular PC by hovering marks at the same points, as shown in

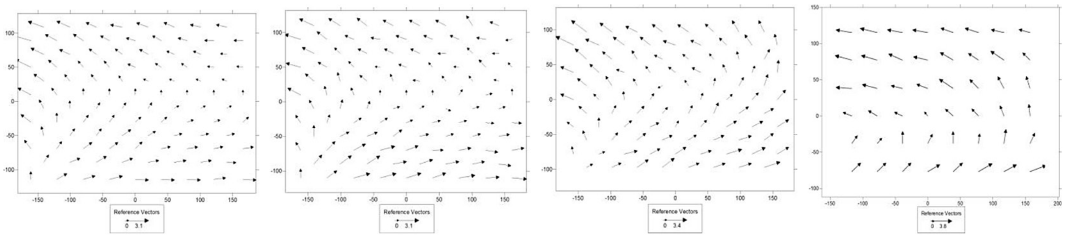

a) M = 2500^x b) M = 5000^x c) M = 10000^x d) M = 20000^x

Figure 2. Vector diagrams of geometric distortions of digital SEM images of the test object with r = 1425 lines/mm at different increases M^x to approximation

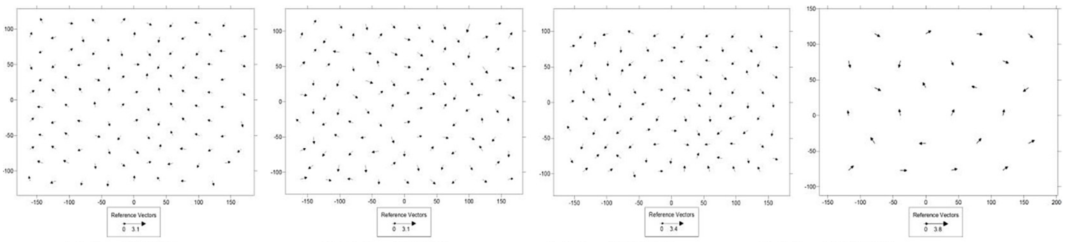

a) M = 2500^x b) M = 5000^x c) M = 10000^x d) M = 20000^x

Figure 3. Vector diagrams of geometric distortions of digital SEM images of the test object with r = 1425 lines/mm at different increases in M^x after approximation

Figure 4. Stereo pair of micro soil of forest soil, obtained on SEM Hitachi S-800 at M = 1000x and angles of inclination of the goniometric table $\alpha_l = 0°$, $\alpha_r = +8°$

the left and right images of the stereo pair. A total of 950 characteristic points of the selected area of the experimental micro soil of forest soil were measured, 850 of which were used to build digital models of surface microrelief by various mathematical methods, and 100 - to control the accuracy of modeling (evenly distributed points did not participate in interpolation and building the 3D model). The size of the scanning area is 105 × 93.3 μm, the area is S = 9800 μm^2 (0.0098 mm^2). The calculation of the spatial coordinates of the measured points is performed according to formulas (1) of the normal case of shooting ($\alpha l = 0°$, $\alpha r \neq 0°$):

$$\left.\begin{aligned} X &= \frac{x_l^0 \cdot 10^3}{M_x}; \\ Y &= \frac{y_l^0 \cdot 10^3}{M_y}; \\ Z(h) &= \frac{x_l^0 \cdot (1 - Cos\alpha_r) + \Delta p_x^0}{M_x \cdot Sin\alpha_r} \cdot 10^3 \end{aligned}\right\} \quad (1)$$

In formulas (1, 2):

$$\left.\begin{aligned} x_l^0 &= x_{l_m} - \Delta x_l, \Delta p_{x_i}^0 = p_{x_i}^0 - p_0, \\ y_l^0 &= y_{l_m} - \Delta y_l, p_{x_i}^0 = x_{i_l}^0 - x_{i_r}^0. \end{aligned}\right\} \quad (2)$$

With the help of reference test objects (test grids, diffraction gratings) it is possible to determine the parameters of the actual magnifications

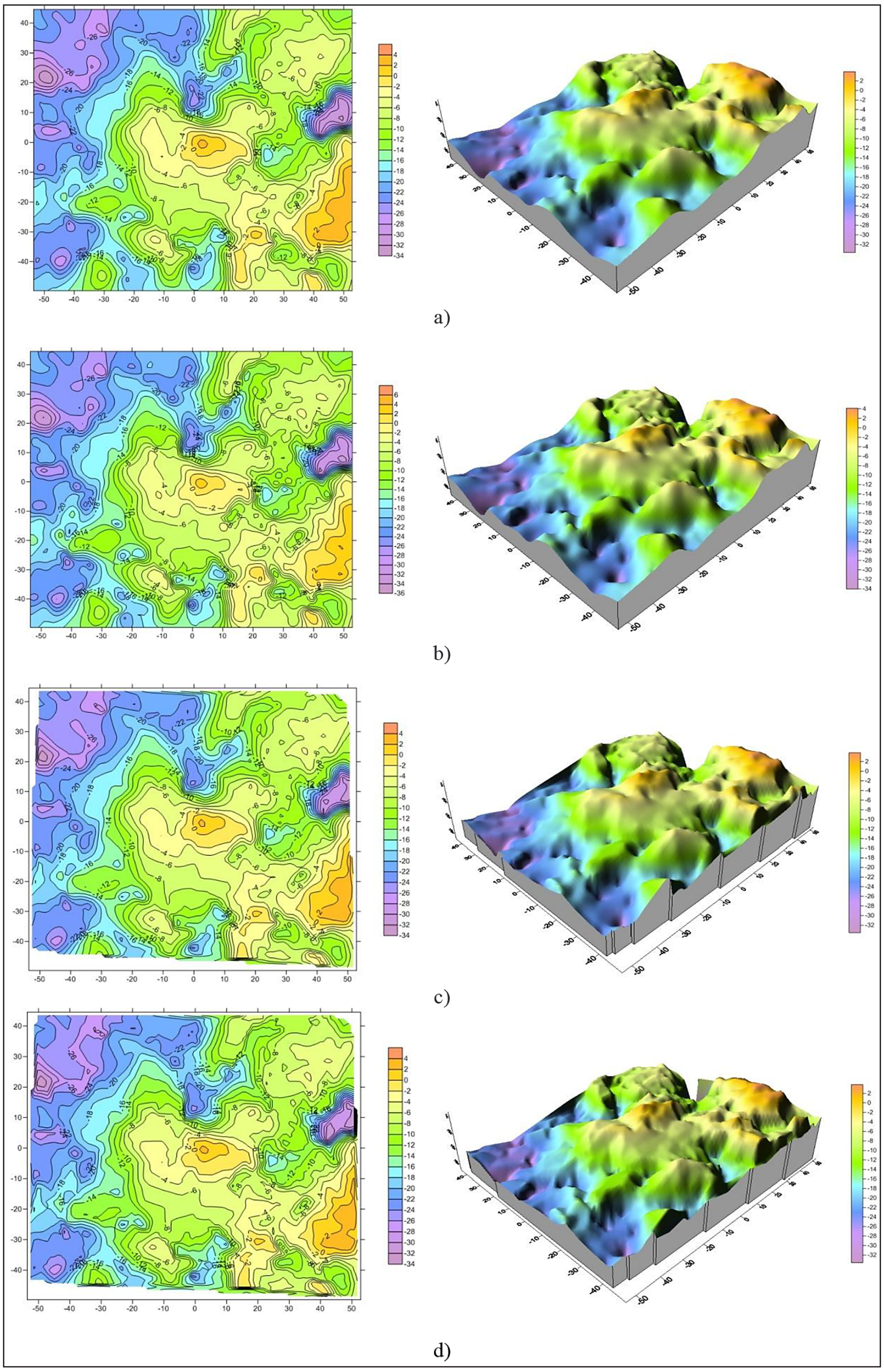

Figure 5. Examples of graphical representation of the micro soil of forest soil in the form of microplanes and 3D models, built by various mathematical methods on 850 measured points; (a) kringing (linear variogram), (b) RBF, multiquadric method, (c) natural neighbor, (d) triangulation with linear interpolation

of the SEM image Mx, My, as well as the values of geometric distortions of the measured coordinates Δx, Δy, which are best described by polynomials of general degree taking into account:

$$\left.\begin{aligned} \Delta x_l &= a_o + a_1 x_l + a_2 y_l + a_3 x_l y_l + a_4 x_l^2 + \\ &+ a_5 y_l^2 + a_6 x_l^3 + a_7 x_л^2 y_l + a_8 x_l y_l^2 + a_9 y_l^3 \\ \Delta y_l &= b_o + b_1 x_l + b_2 y_l + b_3 x_l y_l + b_4 x_l^2 + \\ &+ b_5 y_l^2 + b_6 x_l^3 + b_7 x_l^2 y_l + b_8 x_l y_l^2 + b_9 y_l^3 \end{aligned}\right\} \quad (3)$$

In formulas (1–3): X, Y, $Z(h)$ – spatial coordinates of microsurface points, μm; $xl_{m,}$ yl_{m} – measured at the digital station coordinates of the points on the left SEM image, mm; xl^{o}, yl^{o} – corrected for geometric distortions Δx, Δy coordinates of points on the left SEM image, mm; ai, bi – coefficients of the polynomial of general form (i = 0, 1, 2, ... 9); Δpx^{o} – the difference between the parallaxes of the *i*-th point pi^{o} and the initial (central) point of the SEM image *po*, mm; *Mx*, *My* – magnification (times) or the scale of the SEM image along the *x*, *y* axes. Before measuring the SEM stereopairs of the forest soil microsurface, the actual values of image magnifications, magnitudes of their geometric distortions were determined using the measurements of the reference test grid with a resolution of r = 200 lines/mm and coefficients of approximate polynomial of the third degree *ai*, *bi* were obtained. This made it possible to take into account the geometric distortions of the images, i.e. to correct the measured coordinates Δx_i, Δy_i and obtain corrected spatial coordinates of the points of the experimental surface *Xi*, *Yi*, *Zi* with accuracy $m_{X,Y}$ = ~ 0.1 µm, $m_Z(h)$ = ~ 1.0 µm, which fully satisfies researchers.

Construction of digital models, microplanes and 3D models

Obtaining a digital model of the microrelief (DMMR) of the research surface was carried out using the Surfer program. Initially, a regular grid of 100 × 90 points with the size of the elementary bed ~ 1 × 1 µm was created according to the measured coordinates of 850 characteristic points of the surface microrelief, in the nodes of which the heights were determined by various interpolation methods. Studies [43, 52] have shown that the highest accuracy of digital modeling for this type of relief is given by kriging methods, radial basis functions, natural neighbor method and triangulation with linear interpolation. The accuracy of modeling the heights of microsurface points by these methods [52] was determined by 100 control points that did not participate in the simulation and it is $m_{Z(h)}$ = 0.7 ÷ 1.0 µm. Figure 5 shows examples of graphical representation of the micro soil of forest soil in the form of microplanes and 3D models.

CONCLUSIONS

The proposed method of photogrammetric processing of SEM images of microsurfaces of research objects is effective and allows obtaining their quantitative spatial parameters with the required accuracy. The conducted research is also distinguished by the lack of use of 3D surface modeling programs, dedicated mainly to typical optical photogrammetry. These programs are not compatible with SEM optics (almost rectangular projection for each pixel obtained), so all processes cannot be carried out automatically. The SEM image settings must be monitored step by step. The accuracy of obtaining the spatial coordinates of the points of microsurfaces depends on the parameters of SEM-shooting – the magnitude of magnification and angles of inclination of the goniometric table when receiving SEM-stereo pairs. In particular, at increases:

- M = 1000x - $m_{X,Y}$ = ~ 0.1 µm, $m_{Z(h)}$ = ~ 1.0 µm,
- M = 10000x - $m_{X,Y}$ = ~ 0.02 µm, $m_{Z(h)}$ = ~ 0.2 µm,
- M = 25000x - $m_{X,Y}$ = ~ 0.01 µm, $m_{Z(h)}$ = ~ 0.1 µm.

During the conducted studies, the authors found that the scale (magnification) of the SEM image affects the accuracy of obtaining spatial coordinates of microsurface points: the larger it is, the greater the accuracy. Increasing the angle of inclination of the right image with respect to the left (horizontal) also increases the accuracy of obtaining spatial coordinates, but not significantly. The flatter the microsurface sculpture is, the greater the angle of inclination of the right image of the stereoscopic pair should be.

Spatial quantitative information about the micro surface of forest soils allows obtaining their physical and mechanical properties, structure, resistance to erosion, which are important in the construction industry and environmental protection. In the course of the research, the authors noted that the type of soil probably does not affect the accuracy of modeling, but only the correctness of the selection of characteristic points of the microrelief of the experimental surface and their number during measurement, as well as the selection of the interpolation method of the obtained spatial coordinates of the microsurface; however, further research would be recommended to confirm this.

The unique approach and use of the Dimicros package and Surfer software gave the expected results. The obtained coordinates meet the assumed accuracy, and Surfer software allowed generating accurate 3D models and microplanes.

This technique can be used in microelectronics, mechanical engineering and aircraft, in nanotechnology industries, where quantitative spatial information about the micro surface of objects at the micro level can improve the quality of their manufacture and thus increase the efficiency of modern industry.

REFERENCES

1. Jaidka S., Sharma R., Kaur S., Singh D.P. Scanning electron microscopy (SEM): Learning to generate and interpret the topographical aspects of materials. Microscopic Techniques for the Non-Expert. Springer International Publishing; 2022; 165–85. https://doi.org/10.1007/978-3-030-99542-3_7
2. Ahamad M.S.S., Maizul E.N.M. Digital analysis of geo-referenced concrete Scanning Electron Microscope (SEM) images. Civil and Environmental Engineering Reports. 2020; 30(2). https://doi.org/10.2478/ceer-2020-0020
3. Newell T., Tillotson B., Pearl H., Miller A. Detection of electrical defects with SEMVision in semiconductor production mode manufacturing. In: 2016 27th Annual SEMI Advanced Semiconductor Manufacturing Conference (ASMC); 2016; 151–6. Available from: https://ieeexplore.ieee.org/abstract/document/7491149
4. López de la Rosa, F., Sánchez-Reolid, R., Gómez-Sirvent, J.L., Morales, R., Fernández-Caballero, A. A review on machine and deep learning for semiconductor defect classification in scanning electron microscope images. Applied Sciences. 2021; 11(20): 9508. https://doi.org/10.3390/app11209508
5. Kozikowski, P. Extracting three-dimensional information from SEM images by means of photogrammetry. Micron 2020; 134, 102873. https://doi.org/10.1016/j.micron.2020.102873
6. Ball, A. D., Job, P. A., Walker, A. E. SEM-microphotogrammetry, a new take on an old method for generating high-resolution 3D models from SEM images. Journal of microscopy 2017; 267(2), 214–226. https://doi.org/10.1111/jmi.12560
7. Bangaru, S.S., Wang, C., Zhou, X., Hassan, M. Scanning electron microscopy (SEM) image segmentation for microstructure analysis of concrete using U-net convolutional neural network. Automation in Construction. 2022; 144: 104602. https://doi.org/10.1016/j.autcon.2022.104602
8. Shah, K., Sockalingam, S., O'Brien, H., Yang, G., EL Loubani, M., Lee, D., Sutton, M. A. Submicroscale speckle pattern creation on single carbon fibers for scanning electron microscope-digital image correlation (SEM-DIC) experiments. Composites Part A: Applied Science and Manufacturing. 2023; 165: 107331. https://doi.org/10.1016/j.compositesa.2022.107331
9. Sun, X., Brewin, R. J., Hacker, C., Viljoen, J. J., Li, M. Generating open-source 3D phytoplankton models by integrating photogrammetry with scanning electron microscopy. Frontiers in Microbiology 2024; 15, 1429179. https://doi.org/10.3389/fmicb.2024.1429179
10. Wiatr, A., Job, K., Wiatr, M. Pattern of cholesteatomas under a scanning electron microscope - a risk factor for bone resorption. ACTA Otorhinolaryngologica Italica. 2021; 41(4): 371. https://doi.org/10.14639/0392-100X-N1413
11. Yuan, J., Yang, L., Yu, P., Tang, N., Liu, L., Wang, W., et al. Comparison and development of scanning electron microscope techniques for delicate plant tissues. Plant Science. 2024; 340: 111963. https://doi.org/https://doi.org/10.1016/j.plantsci.2023.111963
12. Rickard, W. D., Coelho, J. F. R., Hollick, J., Soon, S., Woods, A. Application of photogrammetric 3D reconstruction to scanning electron microscopy: Considerations for volume analysis. Electronic Imaging 2021; 33, 1–9. https://doi.org/10.2352/J.ImagingSci.Technol.2020.64.6.060404
13. Gontard, L.C., López-Castro, J.D., González-Rovira, L., Vázquez-Martínez, J.M., Varela-Feria, F.M., Marcos, M., et al. Assessment of engineered surfaces roughness by high-resolution 3D SEM photogrammetry. Ultramicroscopy. 2017; 177: 106–114. https://doi.org/10.1016/j.ultramic.2017.03.007
14. Mahato, P.L., Weatherby, T., Ewell, K., Jha, R., Mishra, B. Scanning electron microscope-based evaluation of eggshell quality. Poultry Science. 2024; 103(3):103428. https://doi.org/10.1016/j.psj.2024.103428
15. Bullock, E.S., von der Handt, A., Halfpenny, A. Scanning electron microscopy, electron probe microanalysis, and electron backscatter diffraction in the geological sciences. Treatise on Geochemistry (Third edition). Oxford: Elsevier; 2025; 789–828. https://doi.org/10.1016/B978-0-323-99762-1.00087-5
16. Razmjooei, M.J., O'Regan, M. Improved paired light and scanning electron microscope imaging technique for identifying nannofossils in Arctic sediments. Geobios. 2024; 87: 45–56. https://doi.org/10.1016/j.geobios.2024.08.016
17. Ali, A., Zhang, N., Santos, R.M. Mineral characterization using scanning electron microscopy (SEM): A review of the fundamentals, advancements, and research directions. Applied Sciences (Switzerland). 2023; 13(23). https://doi.org/10.3390/app132312600
18. Barbieri, G., da Silva, F. P. Acquisition of 3D models with submillimeter-sized features from SEM images by use of photogrammetry: A dimensional comparison to microtomography. Micron 2019; 121: 26–32. https://doi.org/10.1016/j.micron.2019.02.013
19. Gerke, K.M., Korostilev, E.V., Romanenko, K.A., Karsanina, M.V. Going submicron in the precise analysis of soil structure: A FIB-SEM imaging study at nanoscale. Geoderma. 2021; 383: 114739. https://doi.org/10.1016/j.geoderma.2020.114739
20. Kim, H., Han, J., Han, T.Y.J. Machine vision-driven automatic recognition of particle size and morphology in SEM images. Nanoscale. 2020; 12(37):

19461–9. https://doi.org/10.1039/D0NR04140H

21. Dahy, G., Soliman, M.M., Alshater, H., Slowik, A., Ella Hassanien A. Optimized deep networks for the classification of nanoparticles in scanning electron microscopy imaging. Computational Materials Science. 2023; 223. https://doi.org/10.1016/j.commatsci.2023.112135
22. Mazur, A., Obroślak, R., Nieścioruk, K., Król, Ż., Gabryszuk, J., Rybicki, R. Analysis of erosion control constructions effectiveness the case of a road gully in Wielkopole (Lublin Upland). J. Ecol. Eng 2016; 17(4): 180–183. https://doi.org/10.12911/22998993/64507
23. Olson, K.R., Jones, R.L. Soil organic carbon and fly-ash distribution in eroded phases of soils in Illinois and Russia. Soil Till. Res. 2005; 81: 143–153. https://doi.org/10.1016/j.still.2004.09.003
24. Ehrhardt, A., Deumlich, D., Gerke, H.H. Soil surface micro-topography by structure-from-motion photogrammetry for monitoring density and erosion dynamics. Front Environ Sci. 2022; 9. https://doi.org/10.3389/fenvs.2021.737702
25. Hladký, J., Novotná, J., Elbl, J., Kynický, J., Juřička, D., Novotná, J., Brtnický, M. Impacts of water erosion on soil physical properties. Acta Univ. Agric. Silvic. Mendelianae Brun 2016; 64: 1523–1527.
26. Olson, K.R., Gennadiyew, A.N., Jones, R.L., Chernyanskii, S. Erosion pattern on cultivated and reforested hillslopes in Moscow Region, Russia. Soil Sci. Soc. Am. J. 2002; 66: 193–201. https://doi.org/10.2136/sssaj2002.1930a
27. Mazur, A. Quantity and quality of surface and subsurface runoff from an eroded loess slope used for agricultural purposes. Water 2018; 10: 1132. https://doi.org/10.3390/w10091132
28. Mazur, A. Losses of chemical nutrients of plants and soil as a result of the outflow of water from the sodded loess slope. Przem. Chem. 2018a; 97(12): 2154–2157. https://doi.org/10.15199/62.2018.12.28. (in Polish).
29. Mazur, A. Surface and subsurface water runoff and selected matter components from the forested loess slope. J. Ecol. Eng. 2018c; 19(6): 259–266. https://doi.org/10.12911/22998993/95092
30. Howell, P. A practical method for the correction of distortions in SEM photogrammetry. In: Proc Of the Annual Scanning Electron Microscope Symposium Chicago, Illinois. 1975; 199–206.
31. Melnyk, V. M., Voloshin, V. V., Tarasyuk, F. P., Blinder, Yu. S. Methods of quantitative charac-teristics of soil microstructure. Visn. Lviv. state un-tu. Geographical series. Lviv 1999; 25: 24–27. (in Ukrainian).
32. Melnyk, V. M., Shostak, A. V. Quantitative stereo-microfractography: monograph. PVD “Tverdynya” Lutsk 2010; 460. (in Ukrainian).
33. Zhou, W., Apkarian, R., Wang, Z. L., Joy, D. Fundamentals of scanning electron microscopy (SEM). Scanning microscopy for nanotechnology: techniques and applications. Springer 2007; 1–40. https://doi.org/10.1007/978-0-387-39620-0_1
34. Frahm, E. Scanning electron microscopy (SEM): Applications in archaeology. Encyclopedia of global archaeology 2014; 6487–6495. https://doi.org/10.1007/978-1-4419-0465-2_341
35. Tafti, A. P., Kirkpatrick, A. B., Alavi, Z., Owen, H. A., Yu, Z. Recent advances in 3D SEM surface reconstruction. Micron 2015; 78, 54–66. https://doi.org/10.1016/j.micron.2015.07.005
36. Cornille, N., Garcia, D., Sutton, M. A., McNeill, S., Orteu, J. J. Automated 3-D reconstruction using a scanning electron microscope. In: SEM conference on experimental and applied mechanics 2003; June, Charlotte.; 2–4.
37. Erol, A. High-Magnification SEM Micrograph of Siloxanes. In: Atomic-force Microscopy and Its Applications. IntechOpen. 2018; 10(6), 2627–2633. https://doi.org/10.1007/s12633-018-9799-y
38. Gontard, L. C., Batista, M., Salguero, J., Calvino, J. J. Three-dimensional chemical mapping using non-destructive SEM and photogrammetry. Scientific Reports 2018; 8(1), 11000. https://doi.org/10.1038/s41598-018-29458-8
39. Tang, C.S., Lin, L., Cheng, Q., Zhu, C., Wang, D.W., Lin, Z.Y., et al. Quantification and characterizing of soil microstructure features by image processing technique. Computers and Geotechnics. 2020; 128: 103817. https://doi.org/10.1016/j.compgeo.2020.103817
40. Kowalik, M.P., Pelowski, F., Lipowiecki, I. Test and comparison of different digitalization techniques for objects with surfaces difficult to scan. Adv Sci Technol Res J. 2024; 19(2): 1–15. https://doi.org/10.12913/22998624/194997
41. Kwieciński, K., Paluch, M., Lisowska, A. Analysis of the dimensional accuracy of point clouds created by photographic scanning. Adv Sci Technol Res J. 2024; 18(6): 121–32. https://doi.org/10.12913/22998624/191430
42. Kozikowski, P. Extracting three-dimensional information from SEM images by means of photogrammetry. Micron. 2020; 134: 102873. https://doi.org/10.1016/j.micron.2020.102873
43. Ivanchuk, O. Technology of processing digital SEM-images of solid microfloors. Urban planning and territorial planning: scientific-technical. coll. KNUBA. Kyiv 2017; 63: 170–184. (in Ukrainian).
44. Ivanchuk, O. Application of the method of photogrammetrical operation of SEM-stereo pairs for investigation of microsurfaces of geological objects and soils. Cadastre, photogrammetry,

geoinformatics: modern technologies and development perspectives: materials of the third international conference, September 26–28, 2001, Kraków, Osieczany. - Archiwum Fotogrametrii, Kartografii i Teledetekcji. Cracow 2001; 11: 5.11–5.18. (in Ukrainian).

45. Ivanchuk, O., Khrupin, I. Structure and functions of the software complex "Dimicros" for processing REM-images on a digital photogrammetric station. Modern achievements of geodetic science and production. Lviv 2012; I(23): 193–197. (in Ukrainian).
46. Ivanchuk, O. Research of accuracy of the actual value of magnification (scale) of digital SEM images generated by SEM JCM-5000 (NeoScope) of firm JEOL. Geodesy, cartography and aerial photography: interdepartmental scientific and technical coll. Lviv 2012; (76): 80–84. (in Ukrainian).
47. Ivanchuk, O., Barfels, T., Heeg, J., Heger, W. Research of values of distortions of digital SEM images obtained on SEM DSM-960A (CARL Zeiss, Germany) and the accuracy of their consideration. Geodesy, cartography and aerial photography: between from. scientific and technical coll. Lviv 2013; 78: 120–126. (in Ukrainian).
48. Boyde, A., Ross, H.F. Photogrammetry and scanning electron microscopy. Photogrammetric Record 1975; 46(8): 408–457. https://doi.org/10.1111/j.1477-9730.1975.tb00805.x
49. Burkhardt, R. Investigations into the calibration of an electron microscope. Mitt. geod. Inst. Techn. Univ. Graz. 1980; 35. (in German).
50. Ghosh S. K., Nagaraja H. Scanning electron micrography and phtogrammetry. Photogrammetric Engineering and Remote Sensing 1976; 5(42): 649–657.
51. Melnyk, V. M., Shostak, A. Fractal theory of soil erosion. Modern achievements of geodetic science and production. Lviv Publishing House Polytechnic 2014; II(28): 78–81.
52. Ivanchuk, O. Research into the accuracy of modeling the microrelief of object surfaces by mathematical methods based on measurements of their digital SEM stereo images. Modern achievements of geodetic science and production. 2015; II(30); 75–81. (in Ukrainian).